LOW VELOCITY IMPACT RESPONSE OF HYBRID PSEUDO-WOVEN FIBER-REINFORCED COMPOSITE LAMINATES

Cyrus Vakili Rad[1*], Frank Thomas[1], Subramani Sockalingam[1], Zafer Gurdal[1]

1: University of South Carolina McNAIR center for aerospace innovation and research
1000 Catawba St.
Columbia, SC 29201

*: Corresponding author

ABSTRACT

Fiber-reinforced composite laminate structures employed in aerospace applications can utilize both woven and unidirectional lamina. While the woven lamina allow for a higher degree of damage tolerance, unidirectional lamina allow for higher stiffness. The utilization of these two lamina types in a hybrid architecture allows the laminate to have high stiffness while also possessing higher damage tolerance. Although these structurally hybridized laminates perform well, other hybrid architectures may offer an improvement of impact and/or compression-after-impact properties, and may lead to easier automation compared to hand-layup architectures used for current hybrid constructions.

An intermediary architecture of woven laminates and unidirectional laminates, coined as pseudo-woven laminates, is proposed as an alternative hybridized structure. Pseudo-woven laminates make use of an *in situ* Automated Fiber Placement (AFP) manufacturing process to produce a unique pseudo-woven architecture. In this study, pseudo-woven laminates are hybridized with unidirectional laminates in an attempt to enhance impact and damage tolerance. Traditional and two different pseudo-woven hybrid laminates were manufactured using carbon fiber reinforced epoxy slit tapes. Laminates are subjected to low velocity drop impact loads to compare their damage tolerance and impact resistance characteristics.

1. INTRODUCTION

Carbon fiber reinforced polymer matrix composite material systems play a critical role in aerospace applications due to their high strength, high stiffness and low density. These composites exhibit brittle failure, limited toughness, and poor damage tolerance [1]. As such, these systems are often overdesigned, thus any increase in damage tolerance can yield significant cost and weight savings. Creating novel composite architectures aided by advanced manufacturing is an attractive approach to enhance toughness and damage tolerance in laminated composites.

3D woven laminates provide through thickness reinforcement and have been shown to prevent delamination, resist crack propagation, and increase impact toughness. 3D woven laminates are shown to have a stepwise fracture in tensile tests and a higher strain than their 2D counterparts. However, 3D woven laminate architecture reduces in-plane tensile strength and stiffness due to the reorientation of fibers [2], [3].

Copyright 2019. Used by the Society of the Advancement of Material and Process Engineering with permission.

SAMPE Conference Proceedings. Charlotte, NC, May 20-23, 2019. Society for the Advancement of Material and Process Engineering – North America.

In this preliminary study, we have manufactured a woven-like composite laminate using unidirectional slit tapes. This laminate architecture uses an *in situ* automated fiber placement (AFP) manufacturing process to selectively place tows at desired locations, creating a woven like architecture, hereafter referred to as pseudo-woven, or PW [2], [3]. Figure 1B serves to schematically illustrate pseudo-woven tow interaction between layers. Figure 1A shows a cured PW laminate where PW subassemblies are combined with traditional layups where woven subassemblies are on the outer surfaces. The PW laminate architecture is hybridized with traditional layups and are subjected to 30 J and 55 J low velocity impact loads to assess impact damage tolerance and resistance when compared to traditionally manufactured control layups.

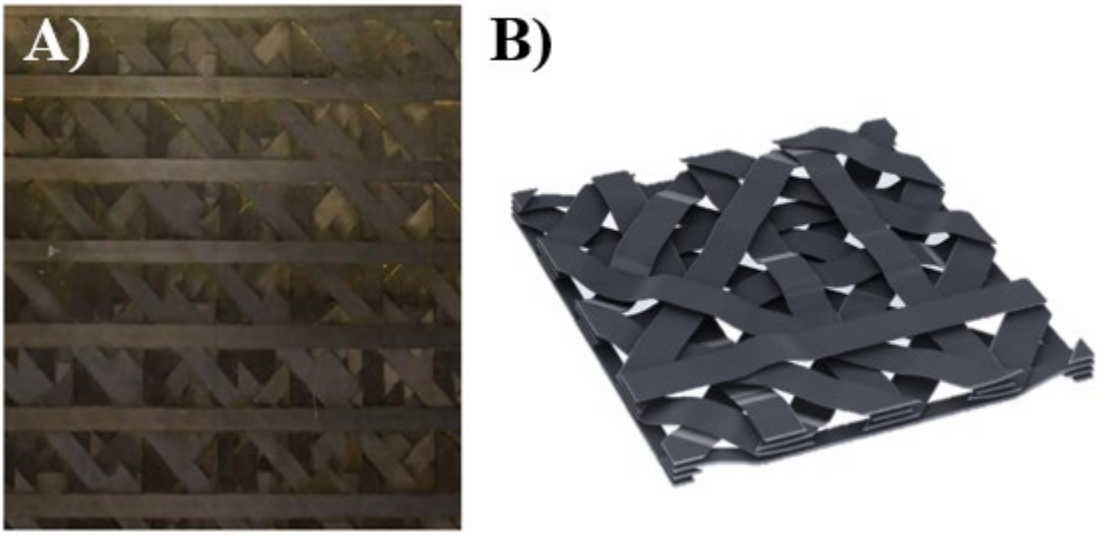


Figure 1. A) Surface of a cured hybrid PW laminate B) schematic illustration of PW architecture [2].

.

2. MANUFACTURING

2.1 Materials

Three laminates configurations are manufactured in this study, two structurally hybridized laminates, one with the PW laminates on the outer surfaces and the other with the PW laminate on the inside, and one control traditional laminate, these layups will be discussed in the coming sections. All laminates manufactured for this study are 24 plies thick and are made with Hexcel IM7G/8552-1 slit tapes cured at 176 °C and 6.2 Bar.

2.2 Pseudo-woven laminates

PW laminates are manufactured through a manipulation of the layup process typically used in AFP manufacturing. Traditionally AFP manufacturing utilizes full tow coverage when laying tows resulting the placement of full bands. When manufacturing a PW laminate, tows are intentionally skipped to produce gaps in the bands, a depiction of full bands and bands with gaps is presented in Figure 2.

Copyright 2019. Used by the Society of the Advancement of Material and Process Engineering with permission.

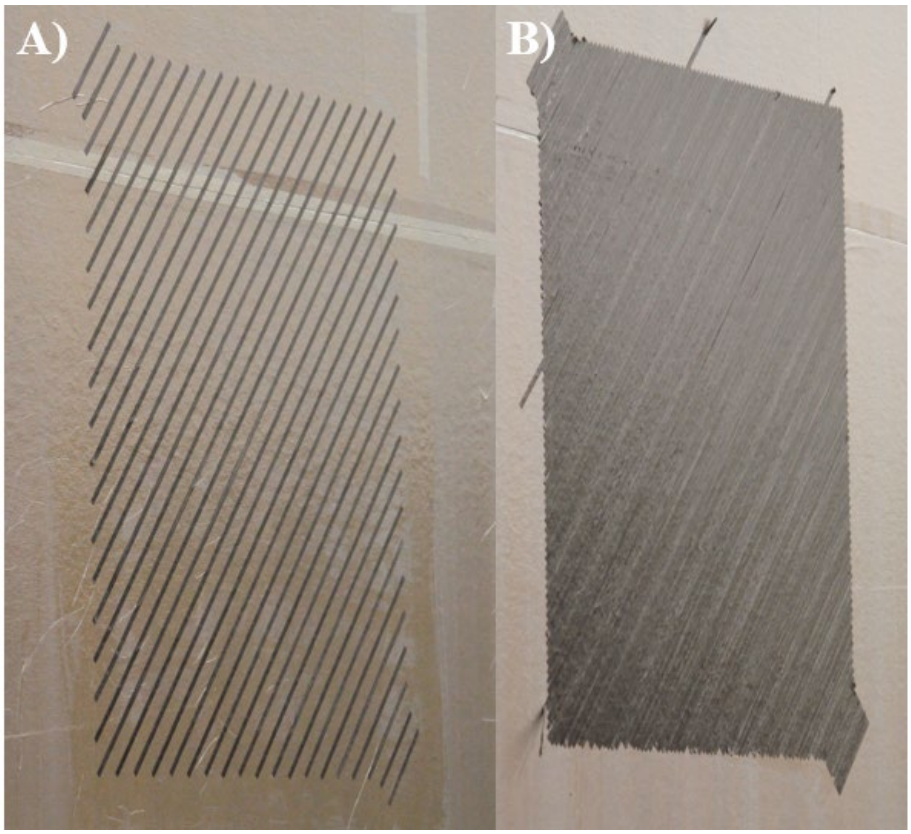


Figure 2. A) A layer with skip tows. B) A layer with no skip tows.

The skipped regions are filled in subsequent passes resulting in a woven-like architecture. This manufacturing process allows for a single tow to occupy multiple positions in the Z coordinate while traditionally manufactured tows do not vary in their Z orientation.

To understand the structure of the PW laminates the manufacture and naming scheme should be discussed. The structure of a PW laminate is described through its AFP notation, this notation provides a format to describe the architecture of a PW laminate and is discussed below. A generic sample of an AFP notation is seen in Figure 3 [2], [4].

$$[\theta^1,\theta^2,\theta^3,\theta^4,..\theta^m]_a[x000x000]_b[w]_c[ds]_d$$

Figure 3. A generic example of AFP notation (a) directional set (b) active channels (c) physical tow width (d) directional shift [3]

AFP notation is broken down into four sections that describe the architecture of a PW laminate. Fig. 3(a) denotes the fiber orientations used in the laminate, this is called the directional set. The directional set provides the order for which orientations are laid. In this example θ^1 is laid, then θ^2

Copyright 2019. Used by the Society of the Advancement of Material and Process Engineering with permission.

to θ^m, where m is the number of fiber angles in the laminate. When referring to PW laminates, a ply is considered as a laid directional set. Figure3(b) shows the tow mask, this serves as a map of active and inactive channels along the AFP's roller, the AFP used for the manufacture of these panels has eight channels. Active channels place tows when the AFP's head makes its passes while inactive channels do not. Active channels are represented as 'x' and inactive as '0', manipulation of the tow channels allows for woven-like architecture to develop. The subscript 'n' on the tow mask denotes the number of times the roller must pass over the domain in each pass to produce a panel of specified width. For example, if the panel is sixteen tows wide then for this eight tow roller, n=2. Note that some layups have two adjacent active channels, these will be referred to as panels with an effective tow width of 12.7 mm. Those with no adjacent active channels will be referred to as having a 6.35 mm effective tow width. Figure 3(c) represents the physical tow width as tow width can vary. Figure 3(d) denotes the directional shift, which takes effect after each directional set has been laid. Once a directional set has been laid, for a directional shift of '1', the first fiber orientation in the previous directional set will shift to the end of the new set thus changing the directional set for the next ply. A representation of directional shift is shown in Table 1, where column A shows the effect of a directional shift of '1', while column B shows a shift of '0'. Note that the tow mask shifts irrespective of directional shift.

Table 1. An example of directional shift effect [3]

	A. Directional shift [1]		B. Directional shift [0]
A) Pass 1	$[\theta^1,\theta^2,\theta^3,\theta^4]$ [x000x000]n [6.35mm][1]	B) Pass 1	$[\theta^1,\theta^2,\theta^3,\theta^4]$ [x000x000]n [6.35mm][0]
A) Pass 2	$[\theta^2,\theta^3,\theta^4,\theta^1]$ [0x000x00]n [6.35mm][1]	B) Pass 2	$[\theta^1,\theta^2,\theta^3,\theta^4]$ [0x000x00]n [6.35mm][0]
A) Pass 3	$[\theta^3,\theta^4,\theta^1,\theta^2]$ [00x000x0]n [6.35mm][1]	B) Pass 3	$[\theta^1,\theta^2,\theta^3,\theta^4]$ [00x000x0]n [6.35mm][0]
A) Pass 4	$[\theta^4,\theta^3,\theta^2,\theta^1]$ [000x000x]n [6.35mm][1]	B) Pass 4	$[\theta^1,\theta^2,\theta^3,\theta^4]$ [000x000x]n [6.35mm][0]

Figure 4(a) illustrates the layup process for a PW laminate used in this study. The AFP notation for the panel is [45, 90,-45,0][x000x000]$_n$[6.35mm][0]. In Figure 4(a) the first directional set is laid onto the tool. The next pass, shown in Figure 4 (b) is laid in the same order as the previous set except the active channel shifts over one space. This process repeats in Figure 4(c) and Figure 4(d) completing the PW laminate assembly.

Copyright 2019. Used by the Society of the Advancement of Material and Process Engineering with permission.

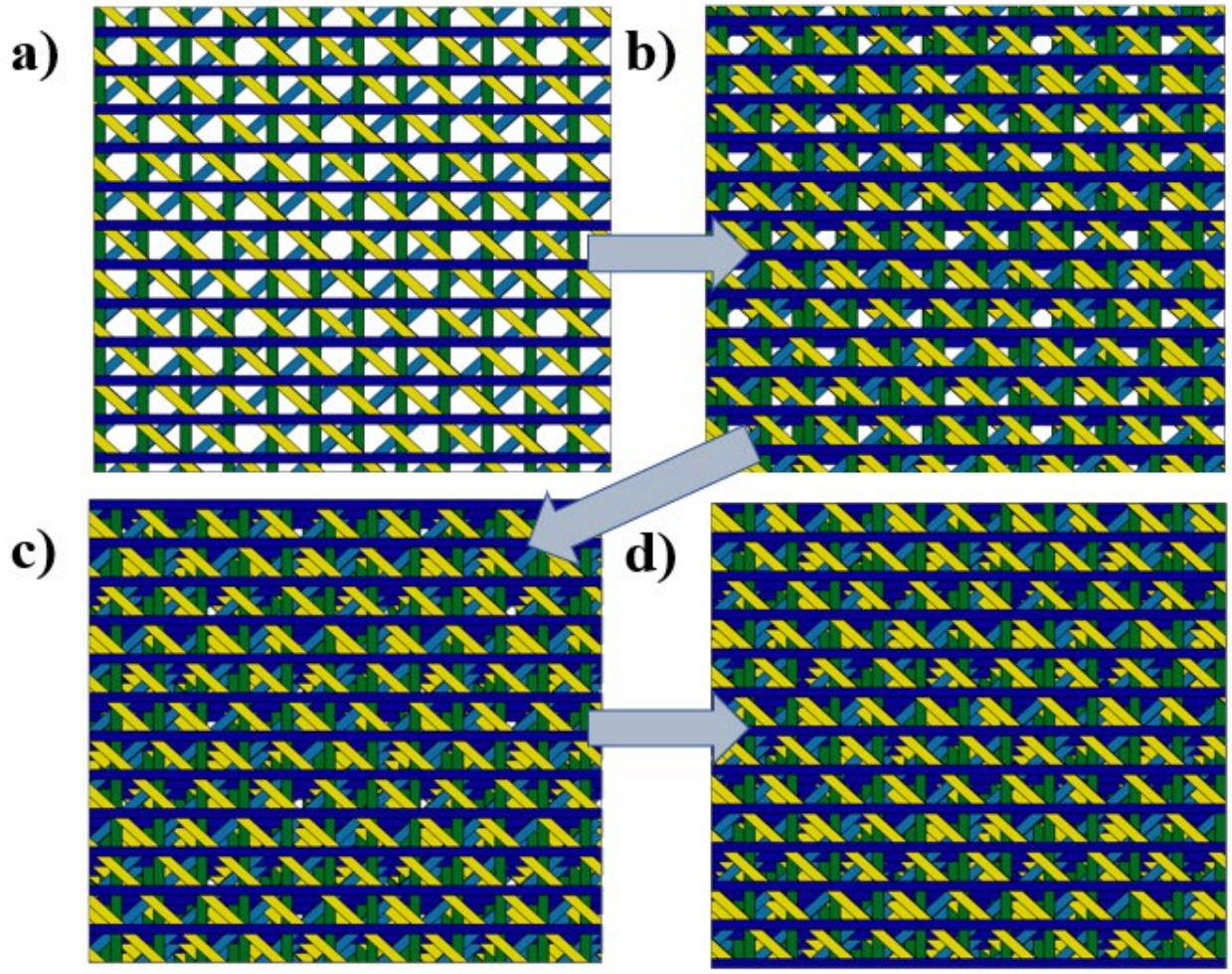


Figure 4**.** A depiction of the manufacturing process a) Pass 1 b) Pass 2 c) Pass 3 d) Pass 4

The naming scheme used for PW laminates is directly representative of their laminate architecture, for example: 3D-DS0-CS6 is a 3 ply laminate whose active channels are side by side producing a double width tow represented as D. The alternative to this would be a single width tow represented as 3S-DS0-CS6 with a S. Directional shift is represented as DS, the number directly following DS is the directional shift. The PW laminates manufactured for this study have a directional shift of 0. CS is the number of channels skipped between active channels, in these laminates three channels are skipped between active channels. The panels manufactured for these experiments are referred to as 4S-DS0-CS3 and INV4S-DS0-CS3. Their AFP notations are [45, 90, -45, 0][x000x000]n[6.35mm][0] and [0, -45, 90, 45][x000x000]n[6.35mm][0] respectively.

2.3 Hybridized panels

The manufacture of PW laminates is a time intensive process, skipping tows during manufacturing increases the time needed to lay up a single ply. For these PW laminates, each ply takes

Copyright 2019. Used by the Society of the Advancement of Material and Process Engineering with permission.

approximately four times longer to lay than a traditional ply because of the skipped tows. As such, hybridizing a traditional laminate structure with PW laminates is used to reduce manufacturing time while gaining insight on PW impact performance. In these experiments two hybrid structures are manufactured, one with the stacking sequence of $[(45/90/-45/0)_2/4S\text{-}DS0\text{-}CS3/INV4S\text{-}DS0\text{-}CS3/(0/-45/90/45)_2]$ where the PW laminates are on the inside, for simplicity, this panel is referred to as Panel 1 or P1. The other panel has the stacking sequence of $[4S\text{-}DS0\text{-}CS3_2/45/90/-45/0/0/-45/90/45/INV4S\text{-}DS0\text{-}CS3_2]$, this panel is referred to as Panel 2 or P2. All panels manufactured for these tests are 24 plies thick including the control sample whose stacking sequence is $[45/90/-45/0]_{3s}$ this panel is referred to as Panel 3 or P3.

3. EXPERIMENTAL

The experimental procedure for the low velocity impact tests is performed in accordance with the ASTM standard D7136. From the three manufactured panels, six 100 mm x 150 mm specimens were extracted from each panel using water jet cutting. To minimize delamination along the edges, panels were fixed onto a wood backing during water jet cutting to prevent vibration. To ensure good edge quality specimens were inspected using a Keyence optical microscope.

Specimens are impacted with a drop tower setup that complies to ASTM standard D7136 a picture of the tower can be seen in Figure 5 the impactor and samples used for these tests are not shown in the setup. Samples were secured with Carr-Lane clamps rated at 1100 N per clamp and were impacted with an instrumented hemispherical impactor cap with a radius of 16 mm. The cart used had a mass of 6.25 kg, this was needed to reach the desired impact energies. Specimens were subjected to impact at 30 J and 55 J, the height needed for the impact energies was calculated using Equation. (1). Where E is the energy level desired, m is the mass, and g is gravity. This results in a drop height of 89.6 mm above the specimen for the 55J impact and 48.9 mm for the 30 J impact.

$$H = \frac{E}{mg} \tag{1}$$

4. RESULTS

All impacted specimens have similar damaged areas and profiles with their respective test group, as such a single specimen is presented for each of the panels at the two energy levels. With one exception to be discussed below. Specimens are named for the panel they originated from as well as their sample number, for example P1S4 is from panel 1 and is sample 4 from that panel. The impact face of select pristine samples are shown in Figure 5. There are 3 samples for panel 1, and 2 samples for panels 2 and 3 tested at 30 J. For 55 J there are three samples for each panel.

Copyright 2019. Used by the Society of the Advancement of Material and Process Engineering with permission.

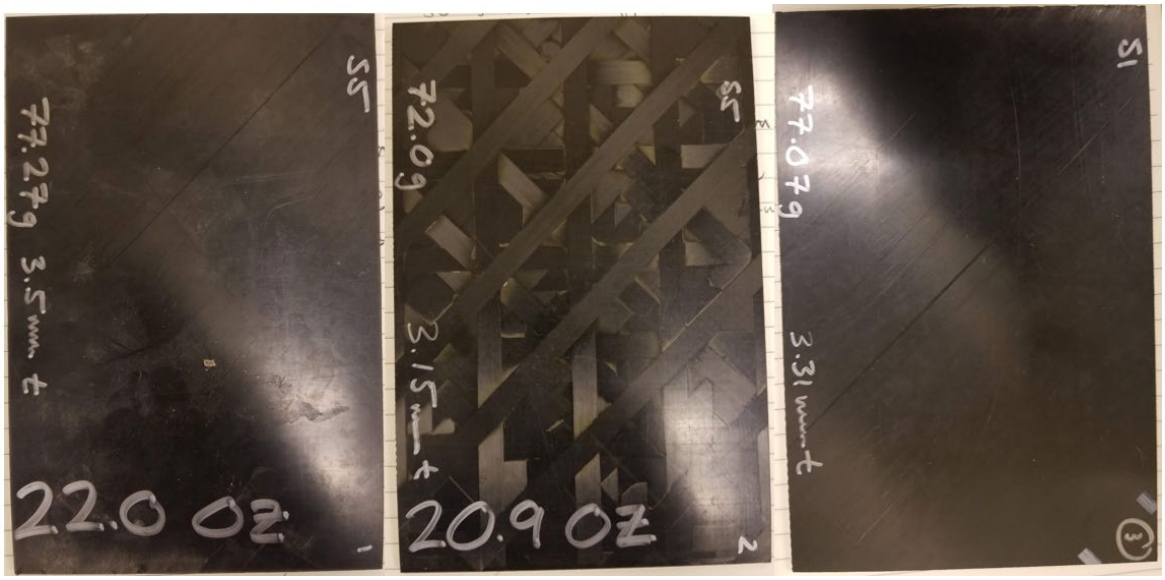


Figure 5. Pristine specimens, from left to right P1S5, P2S5, and P3S1.

All impacted specimens are formatted such that the top left corner is the impact face, the bottom left corner is the back face, and the right side is an angled view. First impacted panels from the 30 J impact energy are shown in Figures 6-8. From these it can be seen that the damaged area for panels 1 and 3 are almost identical to one another while panel 2 shows more localized damage.

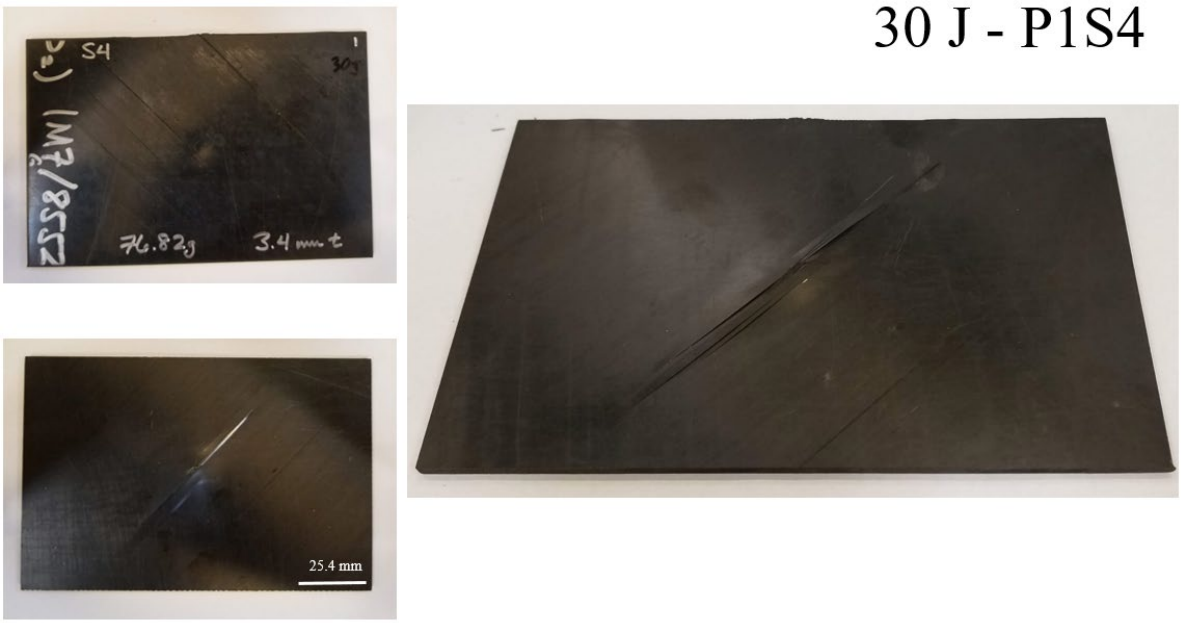


Figure 6. P1S4 30 J impacted specimen, top left: impact face, bottom left: back face, right side: angle view.

Copyright 2019. Used by the Society of the Advancement of Material and Process Engineering with permission.



Figure 7. P2S4 30 J impacted specimen, top left: impact face, bottom left: back face, right side: angle view.

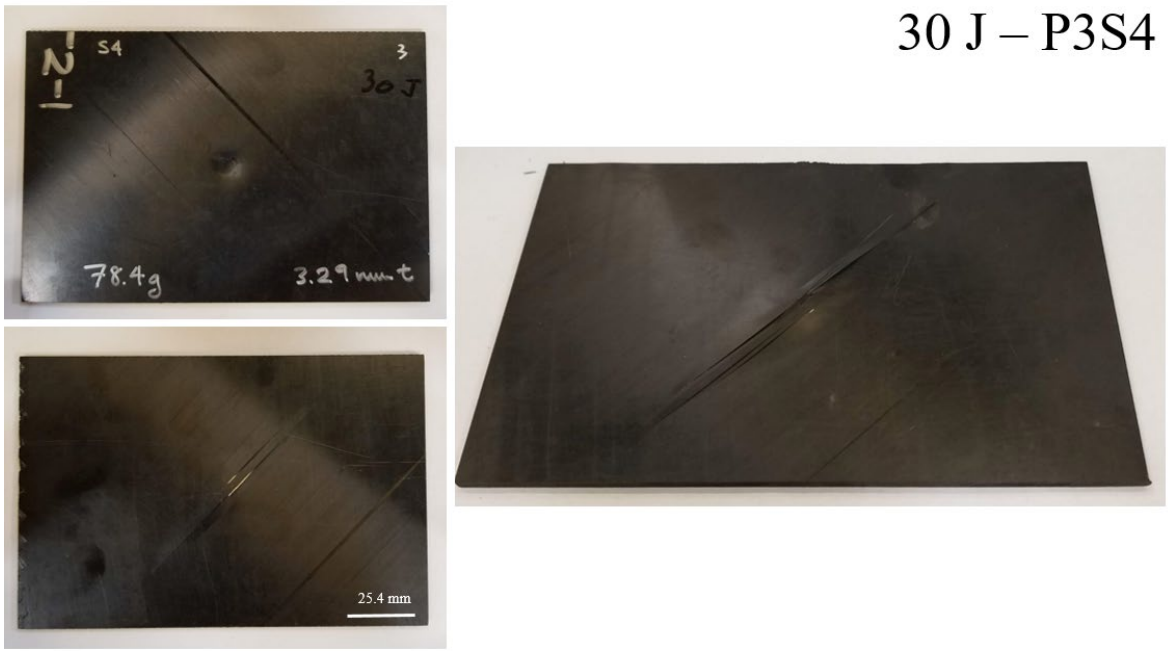


Figure 8. P3S4 30 J impacted specimen, top left: impact face, bottom left: back face, right side: angle view.

Force time and Force displacement plots for the 30 J specimens are presented in Figure 9. For the force time plots panels 1 and 3 behave similarly while panel 2 exhibits a drop in force and then

Copyright 2019. Used by the Society of the Advancement of Material and Process Engineering with permission.

increase in force indicating progressive failure. Force displacement plots show that panel 2 experiences higher displacement compared to other panels and hence absorbs more energy by 15-20% compared to traditional panel 1. The damaged back face for panel 2 is more localized and smaller than that of panels 1 and 3.

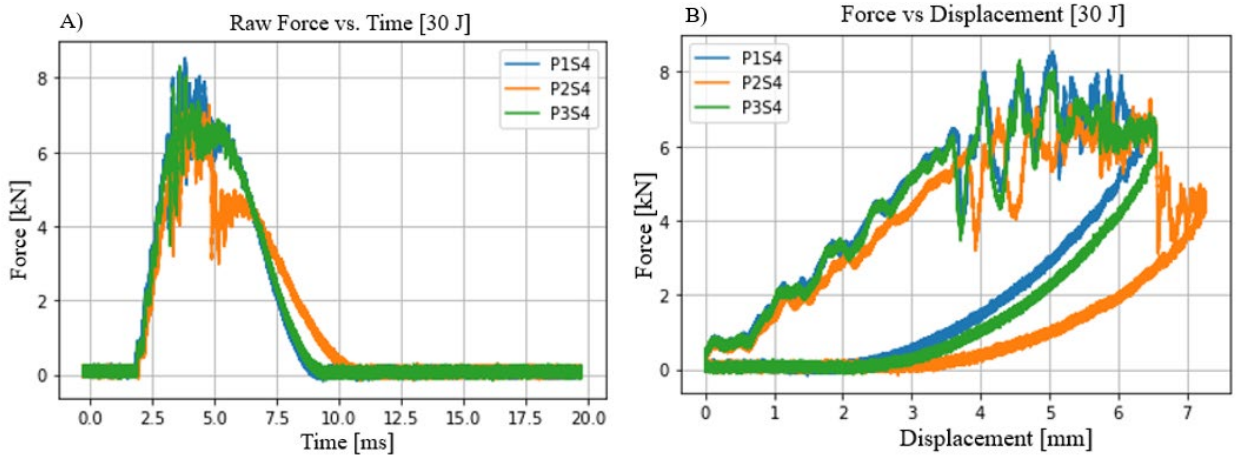
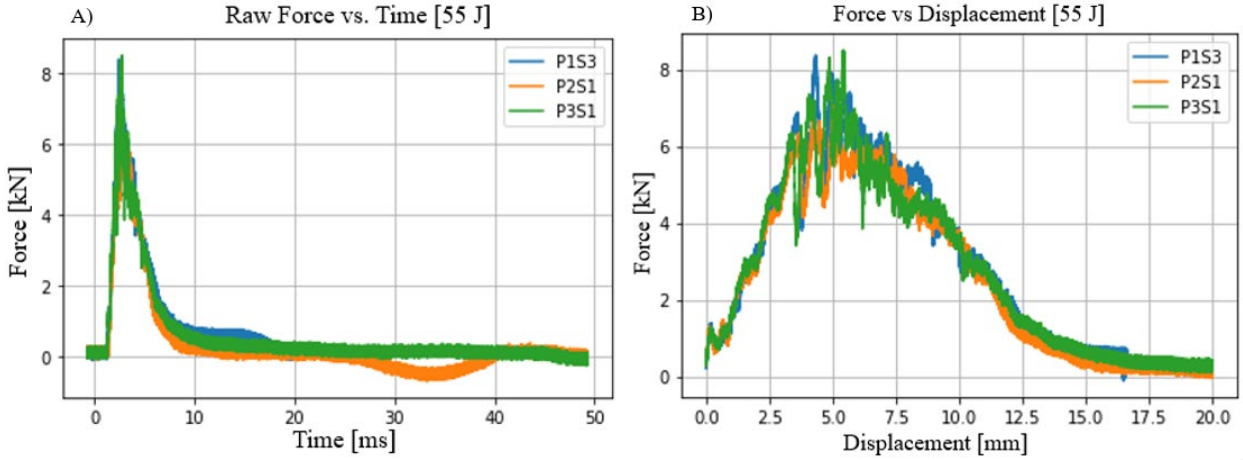


Figure 9. Plots for 30 J impact of A) Force (kN) vs. Time (ms). B) Force (kN) vs Displacement (mm).

The 55 J impact specimens suffered more damage than their 30 J counterparts, with most specimens experiencing penetration. Penetration is defined here as an impact for which the impactor is visible when looking at the back face. Comparing the impacted panels, it can be seen that panel 2's damaged area is smaller than both panels 1 and 3. Only one of the three panel 3 specimens did not show penetration when impacted, while all specimens for the PW hybrid panels showed penetration.

Figure 10 depicts force time and force displacement plots for experimental data at 55 J impact energy. Panels 1 and 3 perform similarly in both plots, while panel 2 exhibits a lower peak force. No retrace is seen as all specimens shown experienced penetration. Maximum force obtained for both 30 J and 55 J impacts are shown for the selected specimens in Table 2.



Copyright 2019. Used by the Society of the Advancement of Material and Process Engineering with permission.

Figure 10**.** Plots for 55 J impact of A) Force (kN) vs. Time (ms). B) Force (kN) vs Displacement (mm).

Table 2. Peak force values for the laminate data selected for 30 J and 55 J impact energies.

Energy Level	Laminate	Max Force (kN)
30 J	P1S4	8.44
	P2S4	7.20
	P3S4	8.23
55 J	P1S3	8.36
	P2S1	6.28
	P3S1	8.40



Figure 11. P1S3 55 J impacted specimen, top left: impact face, bottom left: back face, right side: angle view.

Copyright 2019. Used by the Society of the Advancement of Material and Process Engineering with permission.



Figure 12. P2S1 55 J impacted specimen, top left: impact face, bottom left: back face, right side: angle view.



Figure 13. P3S1 55 J impacted specimen, top left: impact face, bottom left: back face, right side: angle view.

It is interesting to note that in panel 2 impact damage response is dependent upon the impact location. Figure 14 shows the impacted specimen, P2S5. For this specimen impact location falls directly onto a 45 degree tow resulting in a different damage profile from the other panel 2 specimen (Figure 7). The damage profile here more closely resembles the profiles seen in panels 1 and 2.

Copyright 2019. Used by the Society of the Advancement of Material and Process Engineering with permission.



Figure 14. P2S5 30 J impacted specimen, top left: impact face, bottom left: back face, right side: angle view.

CONCLUSIONS

The incorporation of pseudo-woven laminates with traditional laminates to manufacture structurally hybridized laminates significantly reduces the manufacturing time compared to producing thick fully pseudo-woven laminates. Low-velocity impacts are performed on two hybridized specimens and a control specimen. The hybridized configuration where PW laminates are on the outer surfaces exhibited a smaller damaged area than its counterpart's for both 30 J and 55 J impact energies. In addition, the laminates with PW on the outer surfaces absorbed higher energy by 15-20% for 30 J impact compared to other panels. Further investigation is required to determine the effect of PW hybridization on laminate performance and location dependent impact response. The next rounds of testing will explore the effects of lower energy impacts on the hybridized structures.

Acknowledgments

The authors CVR and SS gratefully acknowledge financial support from the SC Space Grant Consortium and the Office of Research University of South Carolina.

Copyright 2019. Used by the Society of the Advancement of Material and Process Engineering with permission.

REFERENCES

[1] Czél, G., Jalalvand, M., Wisnom, MR. "Demonstration of pseudo-ductility in unidirectional hybrid composites made of discontinuous carbon/epoxy and continuous glass/epoxy plies." *Composites Part A* (2015): 75- 84. 10.1016/j.compositesa.2015.01.019.

[2] Vakili Rad, C., Thomas, F., Seay, B., Van Tooren, M., Sockalingam, S. "Manufacturing and characterization of novel clutch non-conventional fiber-reinforced composite laminates." *Composite Structures* (2019). 10.1016/j.compstruct.2019.02.018.

[3] Nagelsmit, M., Kassapoglou, C., Gurdal, Z. "A New Fibre Placement Architecture for Improved Damage Tolerance" (2010).

[4] Van Tooren, M., Sockalingam, S. "Non-conventional composite laminates - clutch laminates." *American Society for Composites*. Philidelphia, Pennsylvania, 2017. Thirty-Second Tech Conf 2017.

[5] Richardson, R.O., Wisheart, M.J., "Review of low-velocity impact properties of composite materials." *Compsites Part A* (1996):1123- 1131. https://doi.org/10.1016/1359-835X(96)00074-7.

[6] Cantwell, W. J., Morton, J. "The impact resistance of composite materials---a review." *Composites* 1991: 347- 362. doi:10.1016/0010-4361(91)90549-V.

[7] ASTM Standard D7136-12, 2012. "Stand Test Method Meas Damage Resist a Fiber-Reinforce Polymer Matrix Composite to a Drop-Weight Impact Event" ASTM International, West Conshohocken, PA, 2010 DOI:10.1520/D7136, www.astm.org

[8] Minakuchi, S., Okabe, Y., Mizutani, T., Takeda, N. "Barely visible impact damage detection for composite sandwich structures by optical-fiber-based distributed strain measurement." Smart Material Structures (2009). 10.1088/0964-1726/18/8/085018.

[9] Aktaş, M., Atas, C., Içten, B. M., Karakuzu, R. "An experimental investigation of the impact response of composite laminates." *Composite Structures* (2009): 307–313. 10.1016/j.compstruct.2008.02.003.

[10] Naik, N.K., Chandra Sekher, Y. "Damage in Laminated Composites Due to Low Velocity Impact." Reinforced Plastic Composites (1998):1232–1263.

Copyright 2019. Used by the Society of the Advancement of Material and Process Engineering with permission.